



Durham Research Online

Deposited in DRO:

21 April 2011

Version of attached file:

Published Version

Peer-review status of attached file:

Peer-reviewed

Citation for published item:

Tanner, B. K. and Wu, H. Z. and Roberts, S. G. (2005) 'Direct evidence for compressive elastic strain at ground surfaces of nanocomposite ceramics.', *Applied physics letters.*, 86 (6). 061909.

Further information on publisher's website:

<http://dx.doi.org/10.1063/1.1862754>

Publisher's copyright statement:

Copyright (2005) American Institute of Physics. This article may be downloaded for personal use only. Any other use requires prior permission of the author and the American Institute of Physics. Tanner, B. K. and Wu, H. Z. and Roberts, S. G. (2005) 'Direct evidence for compressive elastic strain at ground surfaces of nanocomposite ceramics.', *Applied physics letters.*, 86 (6). 061909. and may be found at <http://link.aip.org/link/?apl/86/061909>

Additional information:

Use policy

The full-text may be used and/or reproduced, and given to third parties in any format or medium, without prior permission or charge, for personal research or study, educational, or not-for-profit purposes provided that:

- a full bibliographic reference is made to the original source
- a [link](#) is made to the metadata record in DRO
- the full-text is not changed in any way

The full-text must not be sold in any format or medium without the formal permission of the copyright holders.

Please consult the [full DRO policy](#) for further details.

Direct evidence for compressive elastic strain at ground surfaces of nanocomposite ceramics

B. K. Tanner

Department of Physics, University of Durham, South Road, Durham DH1 3LE, United Kingdom

H. Z. Wu

School of Engineering, Coventry University, Priory Street, Coventry CV15FB, United Kingdom

S. G. Roberts

Department of Materials, University of Oxford, Parks Road, Oxford OX1 3PH, United Kingdom

(Received 14 October 2004; accepted 4 January 2005; published online 3 February 2005)

High-resolution grazing incidence x-ray powder diffraction has been used to provide direct evidence for the existence of a uniform compressive strain close to the surface of ground alumina/SiC nanocomposites. No such strain is found in ground surfaces of single-phase alumina or polished surfaces of nanocomposite. The strain in the ground nanocomposite is found to be perpendicular to the grinding direction and disappears on annealing at 1250 °C. Such a compressive stress provides a mechanism for enhancing the strength of the nanocomposite, by opposing any tensile loading tending to open surface flaws. The origin of the stresses probably lies in the enhanced grain boundary strength in the nanocomposite alumina–silicon carbide compared to alumina. © 2005 American Institute of Physics. [DOI: 10.1063/1.1862754]

The mechanism whereby strengthening occurs in some nanocomposite materials consisting of a brittle matrix within which are embedded nanometer scale particles of a second brittle material is poorly understood. Since the first report of significant strength and toughness improvements in polycrystalline alumina by incorporating a dispersion of 5%–10% submicron silicon carbide particles,¹ some but not all subsequent studies have shown enhanced fracture strength and all have found only small, if any, increases in fracture toughness.^{2–6} The differences in fracture strength between the “nanocomposite” and alumina have been found to depend strongly on the surface finish of the materials.⁷ Although Zhao *et al.*² suggested that strengthening might result from a compressive surface residual stress introduced by the machining, the evidence for this has been limited. Shifts in the Cr³⁺ fluorescence peak in the alumina component of the composites and the minimum fracture load in Hertzian indentation methods have been interpreted in terms of large surface compressive stresses (up to 1500 MPa) being present in ground nanocomposite surfaces but not in ground alumina surfaces.^{7–9} We report here the use of high resolution grazing incidence x-ray powder diffraction to provide direct evidence for the existence of a uniform compressive strain close to the surface of ground alumina/SiC nanocomposites.

Alumina and alumina–silicon carbide nanocomposite samples were produced by a method reported in detail elsewhere.^{5–10} Alumina powder (Sumitomo AKP53) with submicron particle size and quoted chemical purity of 99.99% α -Al₂O₃ was hot pressed at 1500 °C for 1 h under a pressure of 20 MPa. Commercial α -SiC powder (Lonza UF 45) with a mean particle size of \sim 200 nm was mixed with alumina at a concentration of 5% by volume. The nanocomposite was hot pressed in a graphite die at 1650 to 1680 °C for 1 h under 20–25 MPa in flowing argon, resulting in a material with mean grain size of about 3 μ m. An epoxy resin bonded diamond wheel (grit size 150 μ m, wheel speed 1250 rpm, table translation speed 0.8 ms^{–1}, feed depth

12.5 μ m per pass) was used to grind both sides of the hot pressed disks, leaving a specimen thickness of about 3 mm. Selected ground samples were annealed at 1250 °C for 120 min under flowing argon. A reference surface of nanocomposite was produced by fine polishing using a Kent III polishing machine with Engis Kemet plates. The polishing plates rotated at about 60 rpm with an external load of 15 N; diamond grit of 25, 8, 3, and 1 μ m size was used sequentially.

High resolution x-ray powder diffraction enables residual elastic strain to be measured in ceramics from the *shift* in the position of the Bragg diffraction peaks. (We have recently described how the *variation in width* of a selected Bragg peak as a function of the beam incidence angle can be used to measure the strain dispersion, related to the dislocation density, as a function of depth below ground and polished surfaces of alumina and alumina/SiC nanocomposite.¹¹) Precise measurement of the peak maximum of a number of powder diffraction peaks as a function of the (grazing) angle of the incident x-ray beam was undertaken at beamline ID31 at the ESRF, Grenoble. Nine Ge 111 analyzer crystals displaced by 2° with respect to one another permitted rapid parallel data collection at very high resolution.¹² For each incidence angle, the sample remained stationary and the diffraction pattern was recorded by scanning the detectors. The divergence in the scattering plane of the 8 keV incident beam, sagittally focused by a 111 Si monochromator, was 8 arc seconds. For this energy, the Ge analyzer reflection full width at half height maximum (FWHM) was 17 arc seconds giving extremely high angular resolution and strain sensitivity. From an incidence angle of 0.25° to 20°, the penetration depth varied from 0.3 μ m to 25 μ m. The Bragg peaks were fitted to pseudo-Voigt functions. The Bragg angle correction associated with refraction at the surface was determined by measuring the critical angle for total external reflection using a Bede GXR1 reflectometer. As the surfaces were too rough for specular reflectivity measurements, the

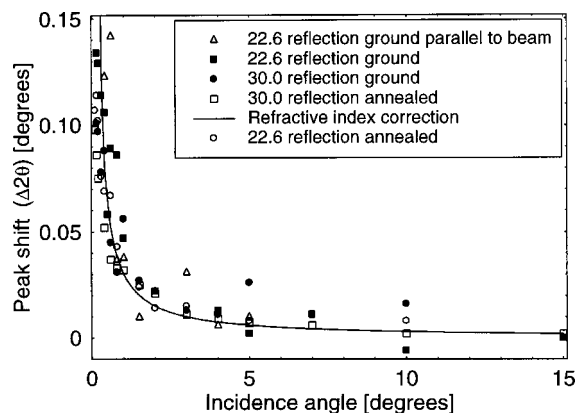


FIG. 1. Displacement of Bragg peak positions, with respect to the values at an incidence angle of 15°, as a function of grazing incidence angle for ground and annealed surfaces of single phase alumina. The solid line is the displacement of the Bragg peak due to refraction.

critical angle was determined from the position of the Yoneda wings in the diffuse scatter recorded from rocking curves at fixed detector angle.¹³

The displacement of the 22.6 and 30.0 Bragg peaks as a function of incidence angle ϕ for ground alumina samples is shown in Fig. 1, together with that for an alumina sample that had been annealed following grinding. The solid line in Fig. 1 is the displacement predicted due to refraction of the incident wave on entering the material. All data lie scattered about this line, indicating that the Bragg plane spacing does not alter as the wave penetrates to progressively smaller depths into the sample with decreasing incidence angle. The absence of a uniform strain in the surface is in marked contrast to the dramatic increase in the full width at half maximum (FWHM) of these Bragg peaks as the incidence angle is reduced.¹¹ Annealing has no effect on the Bragg peak displacement, but causes a major reduction in the FWHM and the rate at which the strain dispersion, and dislocation density, falls with depth into the material.¹¹

In marked contrast to the single phase alumina, the Bragg peaks of the ground nanocomposite shift to a larger Bragg angle than predicted by the refractive index correction (Fig. 2). All reflections for ground nanocomposite surfaces lie well above the line, except for the 30.0 reflection (for the crystal orientation used, the 30.0 planes will not significantly change their spacing in response to an in-plane surface stress, because of Poisson's ratio effects¹¹). The increase in Bragg

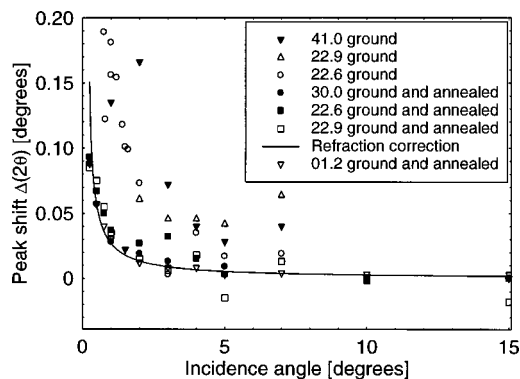


FIG. 2. Displacement of Bragg peak positions as a function of incidence angle for ground and annealed surfaces of alumina/SiC nanocomposite. The solid line is the shift associated with refraction.

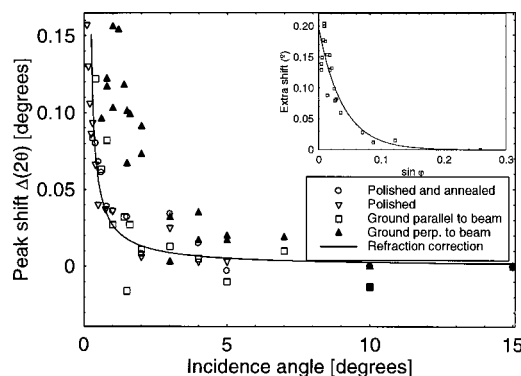


FIG. 3. Displacement of 22.6 Bragg peak positions as a function of incidence angle for ground nanocomposite with grinding direction parallel and perpendicular to the x-ray incidence plane (containing the beam and diffraction vector). The data come from several independent experiments. The inset shows the difference between the measured peak displacement and the refraction correction for the 22.6 reflection (perpendicular to the grinding direction) fitted to an exponential function of the x-ray absorption path length. Also shown are data for polished and for polished annealed nanocomposite.

angle means that the in-plane lattice parameter is decreased; the lattice is compressed. However, on annealing, the uniform strain disappears and all Bragg peaks are displaced only by the value predicted for the refraction correction corresponding to the experimentally measured refractive index.

Deconvolution of the measured peak position as a function of angle to derive the strain as a function of depth is complex due to the strong variation of the FWHM with incidence angle. For higher angles, although the beam probes the scattering deep in the material, scattering from the highly defective near-surface region is convolved into the data. The weighting of the contribution from difference depths therefore depends both on the angular shape and position of the Bragg scatter associated with each elemental slice of material. If we make the very drastic simplification that the Bragg peak position is associated with the average depth of penetration of the x-ray beam, we can extrapolate the surface compressive strain assuming that the strain falls exponentially from the surface. Such a model function provides a very good description of the strain dispersion, and hence Bragg peak FWHM.¹⁴ The scatter on the data is too high to permit a stringent test of the validity of these assumptions but the fit (inset to Fig. 3) is sufficient to extrapolate confidently to a strain induced shift of 0.2° in the scattering angle associated at the surface. This corresponds to a surface compressive strain of $0.1 \pm 0.01\%$, or compressive stress of 400 ± 40 MPa.

Alignment of the ground nanocomposite sample such that the grinding direction lies either in or perpendicular to the incidence plane results in different displacements of the Bragg peaks (Fig. 3). When the grinding direction is perpendicular to the diffraction vector, the peak shift is greater than the refraction correction; when the grinding direction is in the incidence plane, the peak shift drops back to the value predicted for the refraction correction. Thus, for the nanocomposite, the strain is oriented perpendicular to the grinding direction. Figure 1 shows that, in single phase alumina, there is also no evidence of strain when the grinding direction is in the x-ray incidence plane. Scanning electron micrographs of the ground surfaces of the alumina and nanocomposite show dramatically different topologies (Fig. 4). The alumina surface shows little anisotropy but very substantial

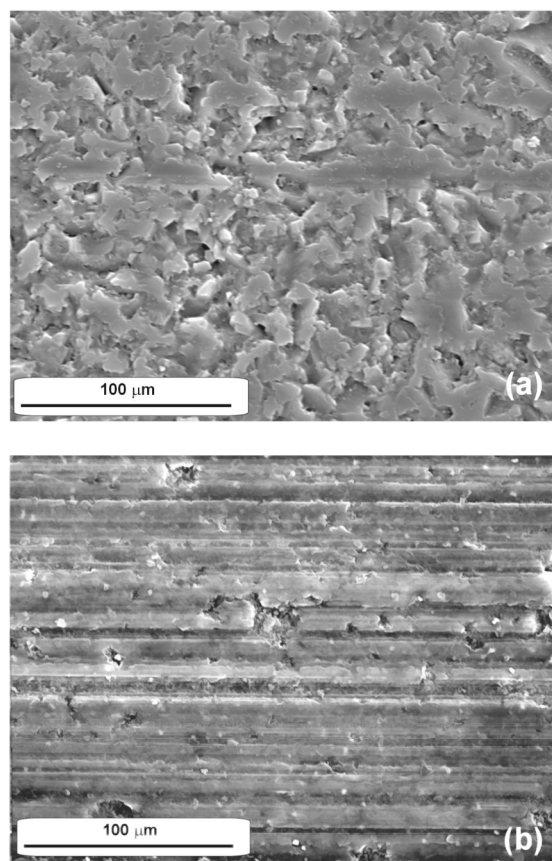


FIG. 4. SEM images of surfaces of (a) Al_2O_3 and (b) $\text{Al}_2\text{O}_3/5 \text{ vol\% SiC}$ nanocomposite after grinding with $150 \mu\text{m}$ diamond grinding wheel. Grinding direction: left to right.

amounts of grain pull out; the nanocomposite surface contains well defined scribe marks and little grain pull out. The x-ray data are consistent with the effect of strain fields of such cylindrical defects in the nanocomposite.

Polishing of the nanocomposite removes the uniform elastic strain in the surface (Fig. 3); the peak displacements correspond to those predicted by the refraction correction. No further change is observed on subsequent annealing of polished material.

Our results on alumina/SiC show that a compressive strain, and hence stress, exists in the ground surface, primarily oriented normal to the grinding direction, as proposed by Marshall *et al.*¹⁵ It disappears on annealing at 1250°C . The strain is not evident in the ground surface of single phase alumina or polished surfaces of nanocomposite. Such a compressive stress provides a mechanism for enhancing the strength of the nanocomposite, by opposing any tensile loading tending to open surface flaws. Since the largest and thus most effective strength-reducing flaws induced by grinding are expected to lie along the grinding direction,¹⁶ the

grinding-induced stress is oriented for the maximum strengthening effect. We have thus direct evidence for the mechanism of Zhao *et al.*² and Wu *et al.*,⁸ by which alumina–silicon carbide nanocomposites can have increased strength compared to alumina despite little or no increase in toughness.

The origin of the stresses reported here is probably associated with enhanced grain boundary strength of the nanocomposite alumina–silicon carbide compared to alumina, producing transgranular rather than intergranular fracture⁶ and suppressing grain pull-out in erosion,¹⁷ abrasion, and polishing.¹⁸ The severe plastic deformation produced in near-surface grains by grinding⁹ will give rise to high grain boundary stresses. In alumina, with relatively weak grain boundaries, these stresses readily lead to grain-boundary fracture and loss of the most deformed material from the surface. In the nanocomposites, with relatively strong grain boundaries, the deformed material is retained, giving rise to the observed high compressive stresses. The micrographs shown in Fig. 4 are consistent with this mechanism; however the reasons for enhanced grain boundary strength in the nanocomposites are still obscure.

Thanks are expressed to Dr. A. N. Fitch and the staff of ID31 at the ESRF for excellent technical support and Alex Pym for assistance with data collection.

¹K. Niihara and A. Nakahira, *Ann. Chim.-Sci. Mater.* **16**, 479 (1991).

²J. H. Zhao, L. C. Stearns, M. P. Harmer, H. M. Chan, G. A. Miller, and R. F. Cook, *J. Am. Ceram. Soc.* **76**, 503 (1993).

³C. E. Borsa, S. Jiao, R. I. Todd, and R. J. Brook, *J. Microsc. (Paris)* **177**, 305 (1995).

⁴R. W. Davidge, P. C. Twigg, and F. L. Riley, *J. Eur. Ceram. Soc.* **16**, 799 (1996).

⁵L. Carroll, M. Sternitzke, and B. Derby, *Acta Metall. Mater.* **44**, 4543 (1996).

⁶J. Perez-Rigueiro, J. Y. Pastor, J. Llorca, M. Elices, P. Miranzo, and J. S. Moya, *Acta Mater.* **46**, 5399 (1998).

⁷H. Z. Wu, S. G. Roberts, and B. Derby, *Acta Mater.* **49**, 507 (2001).

⁸H. Z. Wu, S. G. Roberts, A. J. Winn, and B. Derby, *Mater. Res. Soc. Symp. Proc.* **581**, 303 (2000).

⁹H. Z. Wu, B. J. Inkson, and S. G. Roberts, *J. Microsc.* **201**, 212 (2001).

¹⁰H. Z. Wu, C. W. Lawrence, S. G. Roberts, and B. Derby, *Acta Mater.* **46**, 3839 (1998).

¹¹B. K. Tanner, H. Z. Wu, S. G. Roberts, and T. P. A. Hase, *Philos. Mag.* **84**, 1219 (2004).

¹²A. N. Fitch, *Mater. Sci. Forum* **228**, 219 (1996).

¹³I. Pape, C. W. Lawrence, S. G. Roberts, G. A. D. Briggs, O. V. Kolosov, A. W. Hey, C. F. Paine, and B. K. Tanner, *Philos. Mag. A* **80**, 1913 (2000).

¹⁴B. K. Tanner, T. P. A. Hase, and H. Z. Wu, *Philos. Mag. Lett.* **81**, 351 (2001).

¹⁵D. B. Marshall, A. G. Evans, B. T. Khuri-Yakub, J. W. Tien, and G. S. Kino, *Proc. R. Soc. London, Ser. A* **35A**, 461 (1983).

¹⁶H. H. K. Xu, L. Wei, and S. Jahanmir, *J. Mater. Res.* **10**, 3204 (1995).

¹⁷H. Kara and S. G. Roberts, *J. Mater. Sci.* **37**, 2421 (2002).

¹⁸A. J. Winn and R. I. Todd, *Br. Ceram. Trans.* **98**, 219 (1999).